Available online at www.sciencedirect.com
ScienceDirect
Journal of Sound and Vibration 304 (2007) 570–586
JOURNAL OF SOUND AND VIBRATION
www.elsevier.com/locate/jsvi

Active boundary control of an Euler–Bernoulli beam for generating vibration-free state

Nobuo Tanaka*, Hiroyuki Iwamoto

Department of Aerospace Engineering, Tokyo Metropolitan University, 6-6 Asahigaoka, Hino-city, Tokyo 191-0065 Japan

Received 7 November 2006; accepted 3 March 2007
Available online 27 April 2007

Abstract

This paper presents active boundary control—ABC—of an Euler–Bernoulli beam, which enables one to generate a desired boundary condition at any designated position of a target beam structure, thereby permitting the structure to possess desired properties characterized by the boundary condition. Furthermore, ABC has potential to create a completely vibration-free state in the designated area of a beam. This paper begins by presenting the principle of ABC using a transfer matrix method, the optimal control law of the ABC system being derived. It is found that, in addition to conventional four classical boundary conditions: free, pinned, clamped and sliding support, ABC can generate two more boundary conditions that may not be observed in real systems but realized by ABC. It is also found that as a result of applying ABC to a specific location, including a current conventional boundary of a beam, a completely vibration-free state in the target region of a beam can be realized. Finally, an experiment using an adaptive feedforward control was conducted, demonstrating that ABC enables the generation of a desired boundary condition at the designated location of a target beam, and of a completely vibration-free state of a beam.

1. Introduction

Recent technological developments have increased the need for the design of vibration-free structures, especially in the nano-technology community. A technology road map disclosed recently outlining the requirements for future generations of semiconductors shows that a key technology element, the width of electrical lead wire, is planned to be as narrow as 22 nm, which is the width of only 100 atoms, and in fact no technology is currently able to achieve this target. With a view to realizing future semiconductors having a highly stringent specification, many technological problems must be resolved. Among these, the establishment of nano-infrastructure is essential; not even a micro-vibration is allowed for a semiconductor fabricating machine. As such, it is worth beginning by reviewing the current status of active vibration control technology and assessing its potential to provide the vibration-free environment required for future generation semiconductor designs and similar applications.

Design methodologies for active vibration control of a distributed-parameter structure can be roughly divided into two categories: the modal-based control approach [1–13]. Modal-based control—which can further be classified into two categories: high performance, narrow band high authority control (HAC), and

*Corresponding author. Tel.: +81 42 585 8668; fax: +81 42 585 8668.
E-mail address: ntanaka@cc.tmit.ac.jp (N. Tanaka).

0022-460X/$ - see front matter © 2007 Elsevier Ltd. All rights reserved.
doi:10.1016/j.jsv.2007.03.015

low performance, broad band low authority control (LAC)—is premised on the assumption that all structural modes are excited to some degree. When attempting to suppress the vibration of a distributed parameter structure using HAC, the method encounters difficulty in achieving control because of the generally large number of modes involved; modal-based control theoretically requires as many sensors and actuators as the number of modes to be controlled. Even with advanced control such as H-infinity control [14], μ-synthesis [15] and Linear Matrix Inequality control (LMI) [16], the resulting controller will require an astonishingly large order even for an extremely simple control object. As such, HAC has a limit on the number of structural modes it can deal with. On the contrary, LAC, which is typically implemented using velocity feedback (DVFB) with collocated sensors and actuators [17–19], may treat all structural modes equally; however, it is not able to preferentially damp modes that are more dominant while ignoring modes that are inconsequential to the final result. Active wave control is based on the excitation mechanism of structural modes. By actively suppressing reflected waves produced in a structure, active wave control aims to make all structural modes inactive, rather than augmenting the damping of a structure. It may thus be regarded as imposing the characteristics of an infinite structure, in which no vibration modes occur, onto a finite structure. The active wave control law has been applied to a flexible beam in a restricted frequency range [9,10,13].

This paper presents active boundary control, "ABC", of a beam that allows the generation of a vibration-free state in a designated area of a target structure. The term "boundary control" is already employed in a number of research fields. For instance, the expression is utilized for the purpose of turbulent boundary layer control or laminar flow control in the fluid dynamics field [20–22]. It is also used in vibration control of a flexible cable [23] and a beam [24–27]. In these instances, the boundary of a structure is defined to be the location where a control actuator/sensor can be installed. Thus the term "boundary control", as used previously refers to the control object *per se* or control actuator/sensor placement.

This paper is concerned with active boundary control, ABC, which possesses the following properties: (i) control capability of generating a desired boundary condition at a designated location of a structure, so that the characteristics of a structure governed by the boundary condition may be controlled; (ii) control capability of generating a completely vibration-free state at a designated region of a structure; (iii) actuators/sensors may be placed at any location of the structure. Therefore, the definition of active boundary control presented in the paper is intrinsically different from those used in the past. For the purpose of emphasizing the new concept of ABC presented in this work, a simplistic model with a simple control strategy is employed: a flexible (Euler–Bernoulli) beam controlled by feedforward control. As in all applications of control, if a disturbance reference signal can be obtained then augmentation with a feedforward system will offer advantages. Feedforward active vibration control is not new; what is new is the control law formulation in this paper which, via the use of wave concepts, explicitly targets a modification to the boundary conditions of the structure (and not necessarily via application of the control input at the boundary of the structure as is used in active control of magnetic bearings, for instance). By actively controlling a boundary condition governing the structural modes of a beam, ABC permits the nullification of the beam vibration, and hence differs, in principle, from active wave control [5–13] which is aimed at suppressing reflected waves. By utilizing a transfer matrix method (see Ref. [28], the ABC law is derived using feedforward control. Moreover, in addition to the four classical boundary conditions: free, clamped, pinned and sliding support, ABC allows the generation of two more boundary conditions which may not be observed in real systems, but are realized by ABC. It is found that applying ABC to a specific location, including a current conventional boundary of a beam, a completely vibration-free state—neither progressive waves nor reflected waves exist—can be realized in the designated region of a flexible beam. Finally, an experiment using adaptive feedforward control was conducted, demonstrating that ABC enables one to generate a desired boundary condition at a designated location of a target beam, as well as to produce a completely vibration-free state for a beam.

2. Active boundary control—ABC—of an Euler–Bernoulli beam

2.1. State equation of an Euler–Bernoulli beam

Before proceeding to the theoretical development of an ABC system, three assumptions are employed in this paper: (i) an Euler–Bernoulli beam is used as a target structure; (ii) only flexural vibration of a beam is

considered; (iii) feedforward control is applied. Then, an equation of motion of an Euler–Bernoulli beam lying along the x-axis is written as

$$EI\frac{\partial^4\xi(x,t)}{\partial x^4}+\rho A\frac{\partial^2\xi(x,t)}{\partial x^2}=f(x,t), \tag{1}$$

where (x,t), E, I, A, ρ and $f(x,t)$ are the deflection of the beam, Young's modulus, cross-sectional inertia of area, cross-sectional area, mass density and applied force per unit length, respectively. In the work, the effects of shear deformation and rotary inertia are assumed to be neglected. To solve the partial differential equation, consider first the homogeneous equation; i.e., $f(x,t)=0$. The solution of Eq. (1) is assumed to be written in the form, $\xi(x,t)=\xi(x)\mathrm{e}^{\mathrm{j}\omega t}$ where j and ω are the imaginary unit and the angular frequency, respectively. Then the deflection of a beam $\xi(x)$ satisfies the following ordinary differential equation:

$$\frac{\partial^4\xi(x)}{\partial x^4}-k^4\xi(x)=0, \tag{2}$$

where k is the flexural wavenumber defined as

$$k^4=\frac{\rho A\omega^2}{EI}. \tag{3}$$

A general solution to Eq. (2) is written as

$$-\xi(x)=a_1\mathrm{e}^{-\mathrm{j}kx}+a_2\mathrm{e}^{-kx}+a_3\mathrm{e}^{\mathrm{j}kx}+a_4\mathrm{e}^{kx}, \tag{4}$$

where a_1, a_2, a_3 and a_4 are constants that may be evaluated by the boundary condition properties of a beam.

Having obtained the deflection $\xi(x)$, slope $\theta(x)$, internal bending moment $m(x)$ and internal shear force $q(x)$ may also be derived by the formulae provided in material mechanics, and these state variables may then be expressed in the vector form as

$$\mathbf{z}(x)=\mathbf{B}(x)\mathbf{a}, \tag{5}$$

where the state vector $\mathbf{z}$(x), matrix $\mathbf{B}$(x) and vector $\mathbf{a}$ are defined as

$$\mathbf{z}(x)=\mathrm{col.}\begin{pmatrix}-\xi(x) & \theta(x) & m(x)/EI & q(x)/EI\end{pmatrix}, \tag{6}$$

$$\mathbf{B}(x)=\begin{pmatrix}\mathrm{e}^{-\mathrm{j}kx} & \mathrm{e}^{-kx} & \mathrm{e}^{\mathrm{j}kx} & \mathrm{e}^{kx}\\ -\mathrm{j}k\mathrm{e}^{-\mathrm{j}kx} & -k\mathrm{e}^{-kx} & \mathrm{j}k\mathrm{e}^{\mathrm{j}kx} & k\mathrm{e}^{kx}\\ -k^2\mathrm{e}^{-\mathrm{j}kx} & k^2\mathrm{e}^{-kx} & -k^2\mathrm{e}^{\mathrm{j}kx} & k^2\mathrm{e}^{kx}\\ \mathrm{j}k^3\mathrm{e}^{-\mathrm{j}kx} & -k^3\mathrm{e}^{-kx} & -\mathrm{j}k^3\mathrm{e}^{\mathrm{j}kx} & k^3\mathrm{e}^{kx}\end{pmatrix}, \tag{7}$$

and

$$\mathbf{a}=\mathrm{col.}\begin{pmatrix}a_1 & a_2 & a_3 & a_4\end{pmatrix}, \tag{8}$$

where col. denotes a column vector. The matrix $\mathbf{B}$(x) further expands to

$$\mathbf{B}(x)=\mathbf{K}\mathbf{D}(x), \tag{9}$$

where $\mathbf{K}$, the flexural wavenumber matrix and $\mathbf{D}$(x), the wave transfer matrix, are defined as

$$\mathbf{K}=\begin{pmatrix}1 & 1 & 1 & 1\\ -\mathrm{j}k & -k & \mathrm{j}k & k\\ -k^2 & k^2 & -k^2 & k^2\\ \mathrm{j}k^3 & -k^3 & -\mathrm{j}k^3 & k^3\end{pmatrix}, \tag{10}$$

and

$$\mathbf{D}(x) = \begin{pmatrix} e^{-jkx} & 0 & 0 & 0 \\ 0 & e^{-kx} & 0 & 0 \\ 0 & 0 & e^{jkx} & 0 \\ 0 & 0 & 0 & e^{kx} \end{pmatrix}. \tag{11}$$

Consider a beam element with points $i-1$ and i at both ends of the element as shown in Fig. 1, and for brevity let $\mathbf{z}(x_{i-1})$ and $\mathbf{z}(x_i)$ be $\mathbf{z}_{i-1}$ and $\mathbf{z}_i$, respectively. Then, with a view to describing the relation between these state vectors, it needs to introduce a local coordinate system to these state vectors; with the origin of the local coordinate system at $\mathbf{z}_{i-1}$, $\mathbf{z}_i$ can be expressed as a function of the distance l_i between these two points. Using Eqs. (5) and (9), the state vectors at the points, $i-1$ and i, are given by

$$\mathbf{z}_{i-1} = \mathbf{KD}(0)\mathbf{a} = \mathbf{Ka}, \tag{12}$$

and

$$\mathbf{z}_i = \mathbf{KD}(l_i)\mathbf{a}. \tag{13}$$

Multiplying Eq. (12) by $\mathbf{K}^{-1}$ and substituting the resulting formula into Eq. (13) leads to the state equation of a beam expressed in the form

$$\mathbf{z}_i = \mathbf{KD}(l_i)\mathbf{K}^{-1}\mathbf{z}_{i-1} = \mathbf{T}_{i,i-1}(l_i)\mathbf{z}_{i-1}, \tag{14}$$

where $\mathbf{T}_{i,\,i-1}$ denotes the transfer matrix connecting the points i and $i-1$, and is defined as

$$\mathbf{T}_{i,i-1}(l_i) = \mathbf{KD}(l_i)\mathbf{K}^{-1} = \begin{pmatrix} t_1 & t_4 & t_3 & t_2 \\ k^4 t_2 & t_1 & t_4 & t_3 \\ k^4 t_3 & k^4 t_2 & t_1 & t_4 \\ k^4 t_4 & k^4 t_3 & k^4 t_2 & t_1 \end{pmatrix}, \tag{15}$$

where

$$t_1 = \left(e^{-jkl_i} + e^{-kl_i} + e^{jkl_i} + e^{kl_i}\right)/4, \quad t_2 = \left(-je^{-jkl_i} - e^{-kl_i} + je^{jkl_i} + e^{kl_i}\right)/4k^3,$$
$$t_3 = \left(-e^{-jkl_i} + e^{-kl_i} - e^{jkl_i} + e^{kl_i}\right)/4k^2, \quad t_4 = \left(je^{-jkl_i} - e^{-kl_i} - je^{jkl_i} + e^{kl_i}\right)/4k. \tag{16}$$

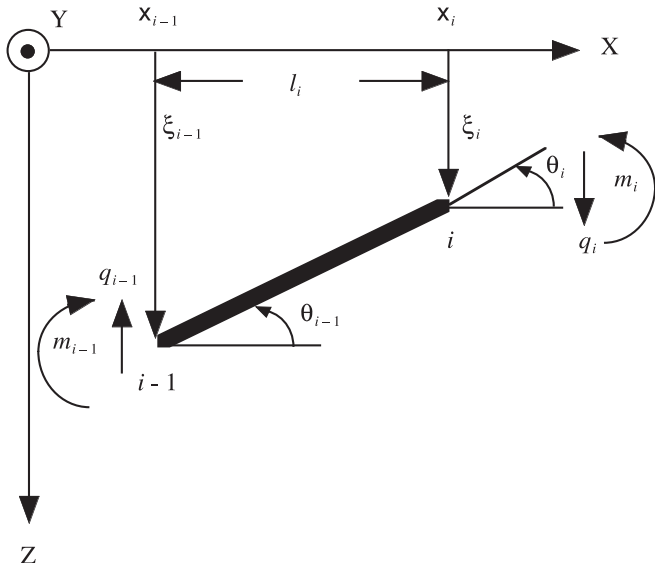

Fig. 1. Coordinate system of an Euler–Bernoulli beam.

Using the flexural wavenumber matrix $\mathbf{K}$, the wave vector $\mathbf{w}$ may be defined as

$$\mathbf{w}(l_i) = \text{col.}\begin{pmatrix} w_1(l_i) & w_2(l_i) & w_3(l_i) & w_4(l_i) \end{pmatrix} = \mathbf{K}^{-1}\mathbf{z}(l_i). \tag{17}$$

Then, substituting the state vectors, $\mathbf{z}(x_{i-1}) = \mathbf{z}_{i-1}$ and $\mathbf{z}(x_i) = \mathbf{z}_i$, and the wave vectors, $\mathbf{w}(x_{i-1}) = \mathbf{w}_{i-1}$ and $\mathbf{w}(x_i) = \mathbf{w}_i$, into Eq. (17) yields

$$\mathbf{w}_i = \mathbf{K}^{-1}\mathbf{T}_{i,i-1}(l_i)\mathbf{K}\mathbf{w}_{i-1} = \mathbf{D}(l_i)\mathbf{w}_{i-1}. \tag{18}$$

As seen from Eq. (18), the matrix $\mathbf{D}$ is found to be the transfer matrix bridging the wave vectors at $i-1$ and i, and hence it is termed the wave transfer matrix.

Clearly from Eqs. (11) and (18), w_1, w_2, w_3 and w_4 are the function of e^{-jkl_i}, e^{-kl_i}, e^{jkl_i}, and e^{kl_i}, respectively. The first wave, w_1, propagates in the positive x direction, while the second term, w_2, decays exponentially as x increases, and thus w_2 is an evanescent wave in the vicinity of the node $i-1$ ($x = 0$). With the same reason, w_3 is a backward propagating wave, while w_4 is an evanescent wave in the vicinity of the node i ($x = l_1$) which decays with distance.

2.2. Control law of the ABC system

Let us derive the control law of an ABC system for generating a desired boundary condition at the designated position of a clamped–clamped beam. Although this paper deals with a clamped–clamped beam as an example, the methodologies presented in the work are still applicable for a flexible beam with other boundary conditions. Note that at conventional boundary conditions of a beam: free ($m = q = 0$), clamped ($\xi = \theta = 0$), pinned ($\xi = m = 0$) and sliding ($\theta = q = 0$), two of the four state variables—ξ, θ, m, q—are always zero, thereby eliminating two out of the four state variables leads to any kind of boundary condition. As such, totally six boundary conditions exist theoretically—two of them: ($\xi = q = 0$) and ($\theta = m = 0$) may not be observed in a real system, however realized by ABC as described later.

In order to conduct ABC, a pair of control forces—combinations of f_c, shear force-type actuator and m_c, bending moment-type actuator as shown in Fig. 2—are required to suppress two state variables independently. Supposing that these control forces act respectively at c_1 and c_2, the control force vectors $\mathbf{f}_{ci}$ ($i = 1, 2$) are given by

For Controller Type 1:

$$\mathbf{f}_{c1} = \text{col.}\begin{pmatrix} 0 & 0 & m_1/EI & 0 \end{pmatrix}, \tag{19}$$

and

$$\mathbf{f}_{c2} = \text{col.}\begin{pmatrix} 0 & 0 & m_2/EI & 0 \end{pmatrix}. \tag{20}$$

For Controller Type 2:

$$\mathbf{f}_{c1} = \text{col.}\begin{pmatrix} 0 & 0 & 0 & f_1/EI \end{pmatrix}, \tag{21}$$

and

$$\mathbf{f}_{c2} = \text{col.}\begin{pmatrix} 0 & 0 & 0 & f_2/EI \end{pmatrix}. \tag{22}$$

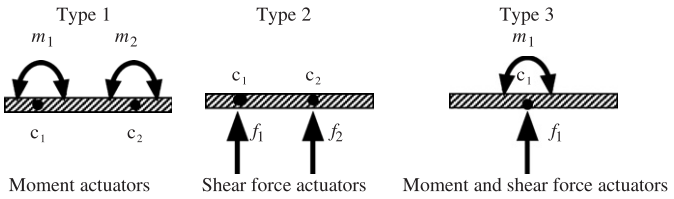

Fig. 2. Controller types.

For Controller Type 3:

$$\mathbf{f}_c = \text{col.}\begin{pmatrix} 0 & 0 & m_1/EI & f_1/EI \end{pmatrix}. \tag{23}$$

Moreover, a disturbance force f_d is assumed to act at d. Then, the disturbance force vector $\mathbf{f}_d$ is similarly written as

$$\mathbf{f}_d = \text{col.}\begin{pmatrix} 0 & 0 & m_d/EI & 0 \end{pmatrix}. \tag{24}$$

To proceed to the theoretical development of an ABC system, this paper adopts the control forces of Type 1 as an example. Furthermore, the state vectors $\mathbf{z}_L$ and $\mathbf{z}_R$ at the left end and right end of a clamped–clamped beam, respectively, are expressed by

$$\mathbf{z}_L = \text{col.}\begin{pmatrix} 0 & 0 & m_L/EI & q_L/EI \end{pmatrix}, \tag{25}$$

and

$$\mathbf{z}_R = \text{col.}\begin{pmatrix} 0 & 0 & m_R/EI & q_R/EI \end{pmatrix}. \tag{26}$$

Using $\mathbf{z}_L$, $\mathbf{f}_{c1}$, $\mathbf{f}_{c2}$ and $\mathbf{f}_d$, the state vector $\mathbf{z}_R$ in Eq. (26) becomes

$$\mathbf{z}_R = \mathbf{T}_{RL}\mathbf{z}_L + \mathbf{T}_{Rc1}\mathbf{f}_{c1} + \mathbf{T}_{Rc2}\mathbf{f}_{c2} + \mathbf{T}_{Rd}\mathbf{f}_d. \tag{27}$$

It is common practice for the transfer matrix method to express the initial state vector $\mathbf{z}_L$—left end of the beam—using all external variables such as m_1, m_2 and f_d. For this purpose, substituting Eqs. (19)–(26) into Eq. (27) enables the state variables m_L and q_L at the left end of the beam to be expressed by

$$\begin{pmatrix} m_L \\ q_L \end{pmatrix} = -\hat{\mathbf{T}}_{RL12}^{-1}\left\{\hat{\mathbf{T}}_{RC_1 12}\begin{pmatrix} m_1 \\ 0 \end{pmatrix} + \hat{\mathbf{T}}_{RC_2 12}\begin{pmatrix} m_2 \\ 0 \end{pmatrix} + \hat{\mathbf{T}}_{Rd12}\begin{pmatrix} m_d \\ 0 \end{pmatrix}\right\} \Big/ EI, \tag{28}$$

where the transfer matrix, $\mathbf{T}_{RL} \in \mathbf{C}^{4\times4}$ is partitioned into four sub-matrices, $\hat{\mathbf{T}}_{RL\,ij} \in \mathbf{C}^{2\times2}$ $(i,j = 1,2)$ such that

$$\mathbf{T}_{RL} = \begin{pmatrix} \hat{\mathbf{T}}_{RL11} & \hat{\mathbf{T}}_{RL12} \\ \hat{\mathbf{T}}_{RL21} & \hat{\mathbf{T}}_{RL22} \end{pmatrix}. \tag{29}$$

Likewise, $\mathbf{T}_{Rc1}$, $\mathbf{T}_{Rc2}$, $\mathbf{T}_{Rd}$ are partitioned into four sub-matrices $\hat{\mathbf{T}}_{RC_1\,ij}$, $\hat{\mathbf{T}}_{RC_2\,ij}$, $\hat{\mathbf{T}}_{Rd\,ij}$ $(i, j = 1, 2)$, respectively.

Let us generate an arbitrary boundary condition at x between the locations c_2 and d (see Fig. 3). To do this, using $\mathbf{z}_L$, $\mathbf{f}_{c1}$ and $\mathbf{f}_{c2}$, the state vector $\mathbf{z}_x$ at x is written as

$$\mathbf{z}_x = \mathbf{T}_{xL}\mathbf{z}_L + \mathbf{T}_{xc1}\mathbf{f}_{c1} + \mathbf{T}_{xc2}\mathbf{f}_{c2}. \tag{30}$$

Eq. (30) further expands to

$$\mathbf{z}_x = \mathbf{A}\begin{pmatrix} m_1 \\ m_2 \end{pmatrix} + \mathbf{b}m_d, \tag{31}$$

where $\mathbf{A} \in \mathbf{C}^{4\times2}$ and $\mathbf{b} \in \mathbf{C}^{4\times1}$ yield

$$\mathbf{A} = \begin{pmatrix} \mathbf{A}_1 & \mathbf{A}_2 \end{pmatrix}, \tag{32}$$

and

$$\mathbf{b} = -\frac{1}{EI}\begin{pmatrix} \hat{\mathbf{T}}_{xL12} \\ \hat{\mathbf{T}}_{xL22} \end{pmatrix}\hat{\mathbf{T}}_{RL12}^{-1}\hat{\mathbf{T}}_{Rd12}\begin{pmatrix} 1 \\ 0 \end{pmatrix}. \tag{33}$$

Here $\mathbf{A}_1 \in \mathbf{C}^{4\times1}$ and $\mathbf{A}_2 \in \mathbf{C}^{4\times1}$ are defined as

$$\mathbf{A}_1 = \left\{\begin{pmatrix} \hat{\mathbf{T}}_{xL12} \\ \hat{\mathbf{T}}_{xL22} \end{pmatrix}\hat{\mathbf{T}}_{RL12}^{-1}\hat{\mathbf{T}}_{RC_1 12} + \frac{1}{EI}\begin{pmatrix} \hat{\mathbf{T}}_{xC_1 12} \\ \hat{\mathbf{T}}_{xC_1 22} \end{pmatrix}\right\}\begin{pmatrix} 1 \\ 0 \end{pmatrix}, \tag{34}$$

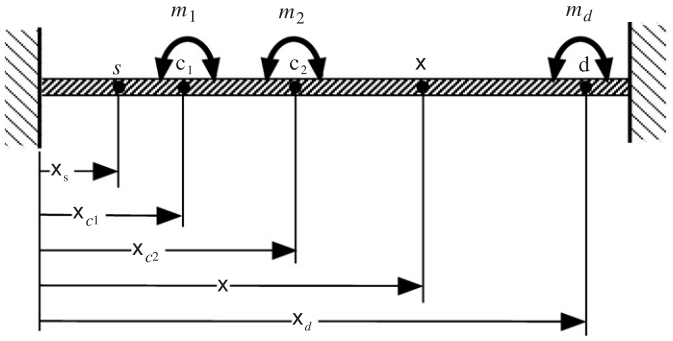

Fig. 3. Beam with control forces and a disturbance force.

and

$$\mathbf{A}_2 = -\left\{ \begin{pmatrix} \hat{\mathbf{T}}_{xL12} \\ \mathbf{T}_{xL} \end{pmatrix} \hat{\mathbf{T}}_{RL12}^{-1} \hat{\mathbf{T}}_{RC_2 12} + \frac{1}{EI} \begin{pmatrix} \hat{\mathbf{T}}_{xC_2 12} \\ \hat{\mathbf{T}}_{xC_2 22} \end{pmatrix} \right\} \begin{pmatrix} 1 \\ 0 \end{pmatrix}. \tag{35}$$

Note again that $\hat{\mathbf{T}}_{xL12}$, $\hat{\mathbf{T}}_{xL22}$ etc., are the sub-matrices partitioned from $\mathbf{T}_{xL}$. Hence, the suppression of two appropriate state variables out of four in $\mathbf{z}_x$ in Eq. (31) generates a desired boundary condition at x. Suppose the ith and jth entries of $\mathbf{z}_x$—for example, $i = 1$ and $j = 2$ refer to a "clamped" support—are to be eliminated. Then, the control law for generating the desired boundary condition at x is described in a form based on the assumption of feedforward control as

$$\begin{pmatrix} m_1 \\ m_2 \end{pmatrix} = -\mathbf{A}_{ij}^{-1} \mathbf{b}_{ij} m_d, \tag{36}$$

where $\mathbf{A}_{ij} \in \mathbf{C}^{2\times 2}$ and $\mathbf{b}_{ij} \in \mathbf{C}^{2\times 1}$ consist of the ith and jth row element(s) of $\mathbf{A}$ and $\mathbf{b}$, respectively.

3. Numerical simulation for generating a boundary condition

Using the controller "Type 1" as shown in Fig. 2, let us generate a desired boundary condition at a designated position x from the left end of a clamped–clamped beam. In a numerical analysis, a pair of moment actuators are placed at $x_{c1} = 0.05$ m and $x_{c2} = 0.2$ m, respectively, the specification of the beam being shown in Table 1. The beam is assumed to be subjected to a disturbance moment m_d acting at $x_d = 1$ m with a sinusoidal moment excitation with the amplitude of 0.0005 Nm.

Fig. 4 illustrates the time histories—before ABC is applied—of four state variables: ξ, θ, m, and q along the x-axis of the beam excited near the third resonance frequency 35.27 Hz. As seen from the figure, the boundary condition "clamped support" at both ends of the beam is justified; that is, ξ and θ are zero whereas m and q are not. As the beam is excited near the third modal frequency, two nodes are observed at one-third and two-thirds of the beam. From the viewpoint of a boundary condition, the nodes possess the characteristics quite similar to a pinned support; both ξ and m are zero (note that under the influence of a near-field effect, the positions where ξ and m become nullified are slightly different), while θ and q are not.

With control forces expressed in Eq. (36), ABC permits one to generate any kind of a desired boundary condition at the designated position of a beam. As an example, consider the case when generating a "clamped support" ($\xi = \theta = 0$) at $x = 0.42$ m of the beam using a pair of moment actuators located at $x_{c1} = 0.05$ m and $x_{c2} = 0.2$ m, respectively. Illustrated in Fig. 5 are the time histories of four state variables of the beam excited near the third modal frequency after ABC. As seen from the figure, both the displacement and slope at the target point $x = 0.42$ m are controlled to be zero, hence a clamped support. The maximum value of the displacement is suppressed to 0.017 mm; 2.32% of the maximum displacement without ABC. It should be noted that as a result of applying ABC for generating a clamped support to the beam, the characteristics of a beam change, and hence the modal frequencies also change. Consequently, the responses of four state

Table 1
Dimensions of a clamped–clamped beam used in numerical analysis

Total length	Thickness	Width
1.1 m	1.5 mm	4.5 cm
Young's modulus	Density	Material
7.4×10^{10} N/m^2	2770 kg/m^3	Duralumin

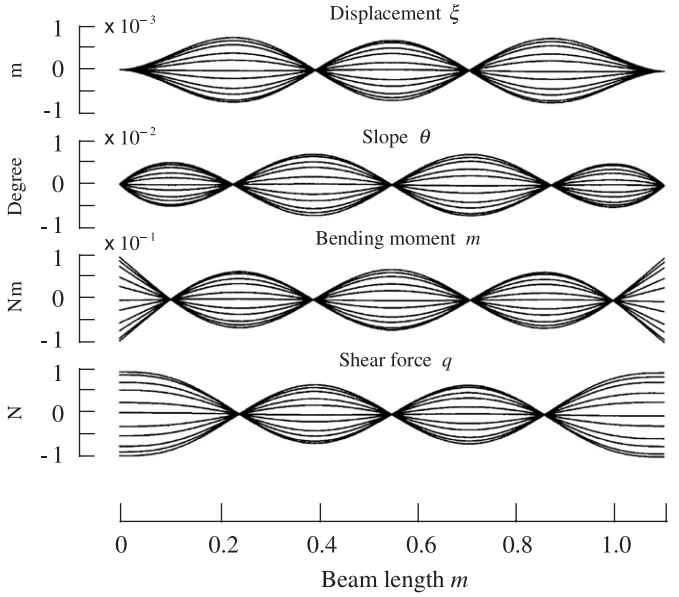

Fig. 4. Time histories of four state variables of a clamped–clamped beam driven near the third resonance frequency, 35.27 Hz.

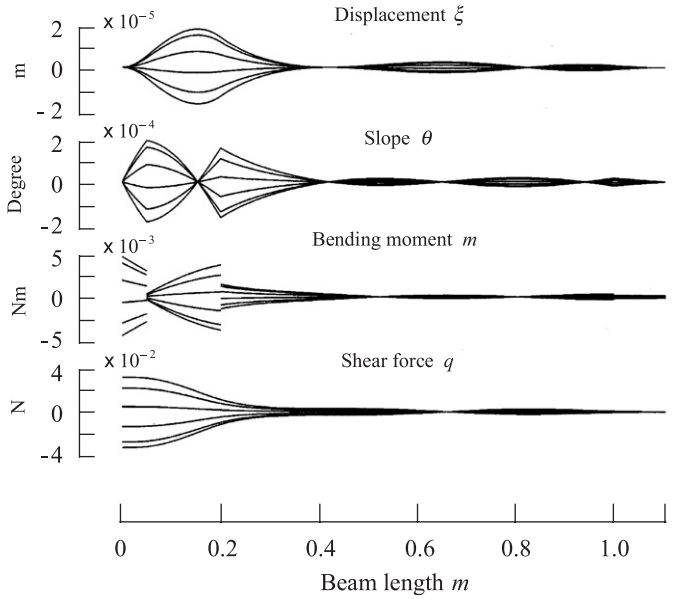

Fig. 5. Time histories of four state variables of a clamped–clamped beam under ABC for generating a clamped support at $x = 0.42$ m.

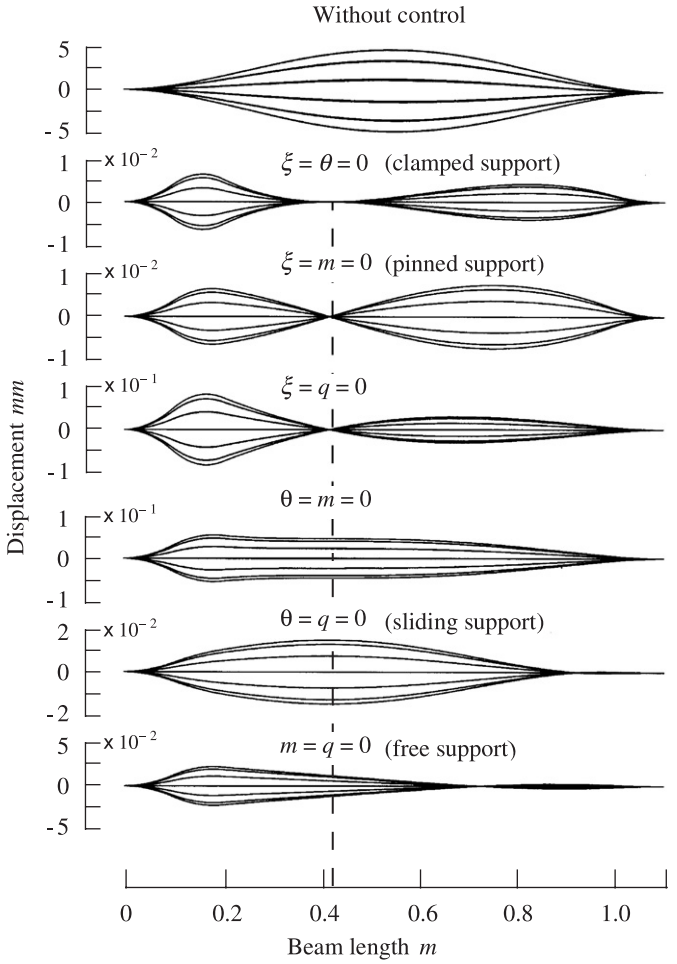

Fig. 6. Time histories of displacement response of a clamped–clamped beam under ABC for generating six kind of boundary support at $x = 0.42$ m.

variables in Fig. 5 vary corresponding to the driving frequency while keeping the designated boundary condition, a clamped support, at the designated location of the beam.

Fig. 6 depicts the time histories of displacement response of the beam after ABC, demonstrating that, in addition to classical four boundary conditions (clamped, free, pinned and sliding support), two more boundary conditions—($\xi = q = 0$) and ($\theta = m = 0$)—are generated at $x = 0.42$ m. The beam in the figure is subjected to a disturbance force acting at $x_d = 1$ m with the driving frequency near the first modal frequency, 6.5 Hz, while a pair of moment controllers act at $x_{c1} = 0.05$ m and $x_{c2} = 0.2$ m, respectively.

4. Generation of a completely vibration-free state using ABC

4.1. What is vibration-free?

It is worth discussing what a vibration-free state is. Take a look again at Fig. 4 where two nodes appear in the time histories of the displacement response of a clamped–clamped beam excited at the third modal frequency 35.27 Hz. It is normally conceived that the nodes are vibration-free so that there have been some attempts to avoid vibration by intentionally designing a way such that a node position coincides with a grip location of a hand-tool. It is true that when placing an accelerometer at a node, the sensor output becomes small; however the node is not vibration-free. A vibration-free state means that all the four state variables

dominating the dynamical characteristics of a beam must be null. Consider an example when a beam, the initial conditions of which are zero, is not subject to any disturbance force. Then no deflection, no slope, no bending moment and no shear force exist along the beam, and hence a whole region of a beam is completely vibration-free.

It is one of the purposes of this paper to generate a vibration-free node via ABC. Then what is the benefit of generating a vibration-free node? To answer this question, consider state vectors $\mathbf{z}_i$ and $\mathbf{z}_j$ at i and j of a beam, respectively. Using a transfer matrix $\mathbf{T}$, the state vector $\mathbf{z}_j$ is related to $\mathbf{z}_i$. Hence it follows that

$$\mathbf{z}_j = \mathbf{T}\mathbf{z}_i. \tag{37}$$

Suppose the state vector $\mathbf{z}_i$ is a null vector, in other words, the node at i is vibration-free, then the state vector $\mathbf{z}_j$ at j apparently becomes a null vector, implying that the area between the points i and j are also vibration-free. Thus, generating a completely vibration-free node at a designated location enables one to produce a vibration-free state around the designated point. Accordingly, the so-called node coming from "no desplacement" where both ξ and m are zero seems to be vibration-free, however other state variables θ and q are non-zero, and hence the state vector at the node is not vibration-free but plays a role of bridging both sides of the node to transfer structural waves.

Another question may arise. How does it differ from a well known DVFB [18,19] with an extremely high feedback gain applied at a sensor/actuator collocated location? The answer is again clear when considering the difference between the so-called node and a vibration-free node. Since the effort of conventional active vibration control including DVFB results in simply producing a node at a sensor location, vibration-free state may not be realized. Even with the control performance for minimizing kinetic energy of a beam being introduced, a vibration-free state may not be realized since the design concept of vibration control is different.

4.2. Completely vibration-free state via ABC

ABC has potential to create a completely vibration-free state in the target region of a beam. Consider a beam with any kind of boundary condition at both ends of the beam with two control forces m_1 and m_2 acting as shown in Fig. 3. The state vector $\mathbf{z}_s$ at s between L, the left end of the beam, and the control point c_1 may be written as

$$\mathbf{z}_S = \mathbf{T}_{SL}\mathbf{z}_L, \tag{38}$$

where the mth element and nth element of $\mathbf{z}_L$ are assumed to be non-zero. When applying ABC to the left end of the beam so as to nullify the two non-zero elements of $\mathbf{z}_L$, the state vector $\mathbf{z}_L$ then becomes a null vector, and hence the state vector $\mathbf{z}_s$ in Eq. (38) becomes also a null vector. As such, all the state variables: ξ, θ, m and q of $\mathbf{z}_s$ become zero, whereby a completely vibration-free state—neither progressive waves nor reflected waves exist—is generated in the region between the left end of the beam and the point s. Note that the point s may be located anywhere between L and the control point c_1, so that in effect the vibration-free state may be produced between L and the control point c_1.

Next, let us apply ABC onto the point at s between the left end of the beam and the control point c_1 (see Fig. 3) in an attempt to assign any kind of boundary condition; say, the kth and lth elements of the state vector $\mathbf{z}_s$ are to be suppressed. Then, Eq. (38) expands to

$$0_k = t_{km}z_{Lm} + t_{kn}z_{Ln}, \tag{39}$$

$$0_l = t_{lm}z_{Lm} + t_{ln}z_{Ln}, \tag{40}$$

where t_{km}, for instance, expresses the kth and mth element of the transfer matrix $\mathbf{T}_{sL}$, and z_{Lm} denotes the mth element of $\mathbf{z}_L$. As seen from Eqs. (39) and (40), the elements, z_{Lm} and z_{Ln}, which are non-zero before ABC are nullified via ABC. Thus, the initial state vector $\mathbf{z}_L$ becomes null, with the result that the state vector between the left end of the beam and the control point c_1 also becomes a null vector, hence vibration-free in the area. In summary, by applying ABC at any location of the beam between the left end of the beam and the control point

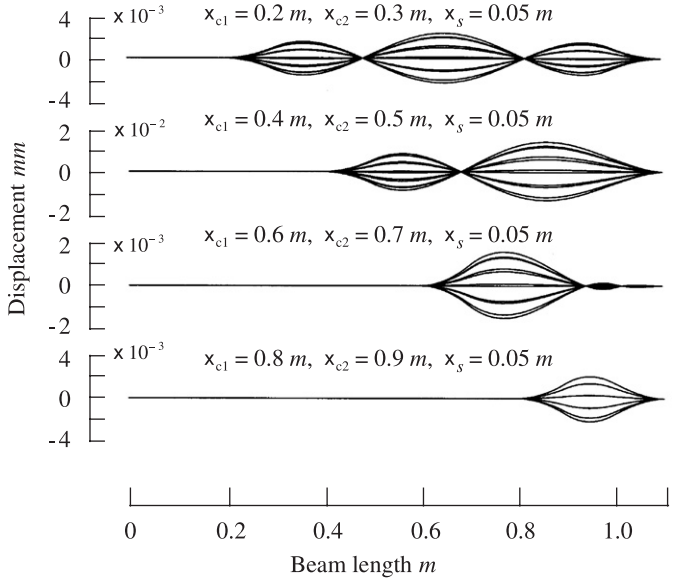

Fig. 7. Time histories of displacement response of a clamped–clamped beam under ABC for generating a completely vibration-free state in the designated region of the beam; control target is $x_s = 0.05$ m.

c_1, including the left end, ABC enables one to generate a completely vibration-free state in the region of a beam by producing *any* kind of boundary condition.

4.3. Numerical simulation for generating a vibration-free state

Illustrated in Fig. 7 are the time histories of displacement response of a clamped–clamped beam after ABC in an effort to generate a clamped support at $x_s = 0.05$ m, with the control locations x_{c1} and x_{c2} varying from 0.2 to 0.8 m, and 0.3 to 0.9 m, respectively, while a disturbance moment m_d acts at $x_d = 1$ m with a sinusoidal moment excitation with the amplitude of 0.0005 Nm.

Clearly from the figure, a completely vibration-free state is generated in the designated region of the beam, albeit the control locations shift. Note that by merely generating *any* kind of boundary condition (clamped support in this case) at *any* place between the left end and x_{c1}, a vibration-free state is generated in between. In order to verify whether it is actually vibration-free or not, other state variables; slope, bending moment and shear force, should also be demonstrated in the figure, however, in light of the definition of the state variables derived by taking the derivative of displacement with respect to x, it is easily understood that these state variables become zero in the region since displacement of a beam is zero from the left end to x_{c1} where a control actuator is positioned. Note that the segment from the actuator location x_{c1} to the right end of the beam is outside the sphere of control. Consequently the properties of the region are characterized by those of a clamped–clamped beam, the effective length of which is shortened as the actuator location shifts toward the right end of the beam. Hence, the effective stiffness of the segment increases so too does the corresponding structure modal frequency.

Fig. 8 shows the time histories of the displacement response of the clamped–clamped beam after ABC with the control locations x_{c1}, x_{c2} and control target location x_s being fixed at 0.6, 0.7 and 0.05 m, respectively, while the driving frequency f of a disturbance force varies from 1 to 50 Hz. As seen from the figure, the beam segment between the left end and x_{c1} becomes completely vibration-free at any driving frequency via ABC. The maximum amplitude of the displacement response in each picture seems to be suppressed; however, as described above the right-hand side of the controller location is beyond the sphere of ABC, so that the suppression of vibration in the segment cannot be expected. Therefore, driving frequency happens to be at off-resonance frequency of a (virtually) shortened segment in this case, hence small amplitude of the displacement response.

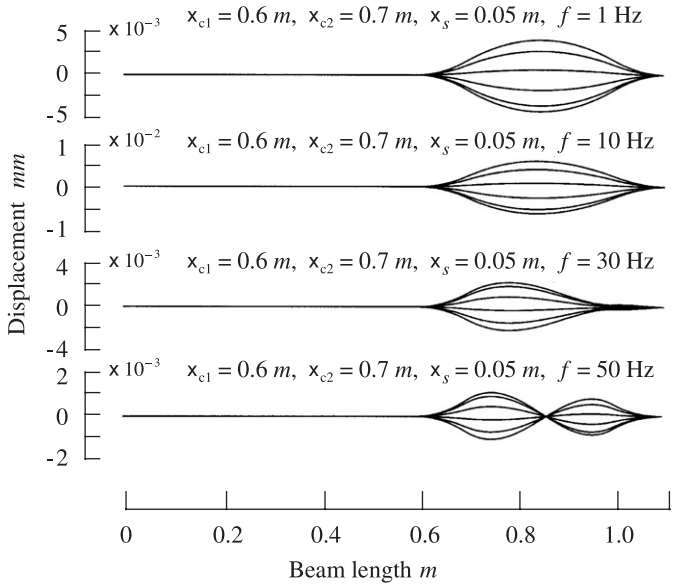

Fig. 8. Time histories of displacement response of a clamped–clamped beam under ABC for generating a completely vibration-free state in the designated region of the beam; driving frequency varies from 1 to 50 Hz.

5. Experiment

5.1. Experimental setup

Feedforward control requires the full knowledge of a target model. Given the full model of a structure, theoretically achievable control effect may be accomplished as shown in Figs. 5–8. If there exists some discrepancy between a mathematical model and a real system, the control effect is deteriorated. When a mathematical model cannot be obtained beforehand, a practical method to cope with this problem may be the use of adaptive feedforward control based upon a filtered-x least mean square (LMS) algorithm. The adaptive feedforward control does not require a mathematical model a priori. Prior to and/or during control, system identification may be conducted to estimate the transfer function between an error sensor and an actuator location. Then, in an effort to minimize an error sensor output, the feedforward control exerts, thereby suppressing unwanted two state variables out of four, and thus producing a new boundary condition at the error sensor location.

Fig. 9 shows a picture of the test rig used in an experiment for the purpose of verifying the validity of ABC for generating a desired boundary condition as well as creating vibration-free state at the designated area of a clamped–clamped beam, the specification of which is the same as used in the numerical analysis (see Table 1). Depicted in Fig. 10 is a schematic diagram of ABC implementation based upon adaptive feedforward control using a filtered-x LMS algorithm. As seen in Figs. 9 and 10, envelopes of a displacement response of the beam were obtained using a wave visualization system that had been developed for this experiment, consisting of a gap sensor array, each sensor being located along the beam with an 8.5 cm interval as shown in Fig. 9. The sensor outputs acquired simultaneously by a data logger were then sent into the wave visualization system to obtain displacement envelopes of the beam. As with a feedforward control strategy using a filtered-x LMS algorithm, two gap sensors were installed at s_1 and s_2 to obtain displacement outputs $\xi(x_{s1})$ and $\xi(x_{s2})$. With these sensor outputs, an average displacement and a slope were estimated by

$$\tilde{\xi} = \frac{\xi(x_{s1}) + \xi(x_{s2})}{2}, \tag{41}$$

and

$$\tilde{\theta} = \frac{\xi(x_{s1}) - \xi(x_{s2})}{x_{s2} - x_{s1}}. \tag{42}$$

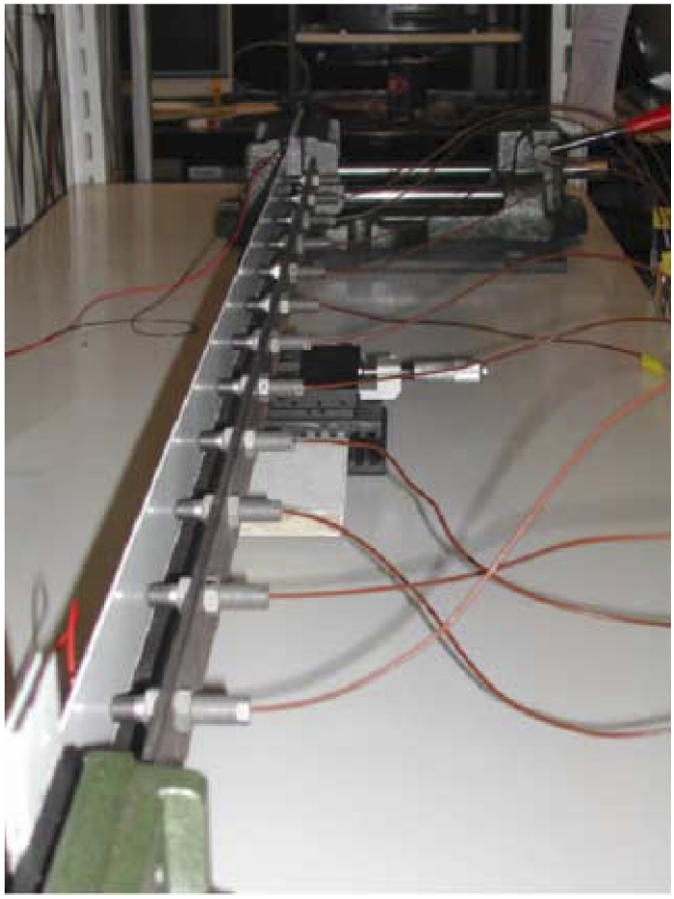

Fig. 9. Outlook of experiment rig.

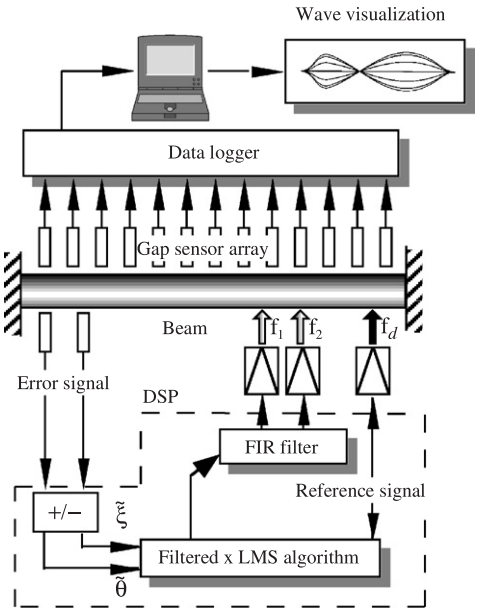

Fig. 10. Schematic diagram of ABC implementation.

These processed signals were then input to an adaptive feedforward control system so as to minimize the squared value of error signal outputs, producing control signals to drive two moment actuators placed at c_1 and c_2.

5.2. Experimental results

Prior to conducting active boundary control experimentally for generating a desired boundary condition at any location of a beam as well as producing a completely vibration-free state at the designated region of the beam, some fundamental characteristics of a target beam were measured. Fig. 11(a) illustrates the envelopes of displacement response of a beam excited at the third modal frequency of 35 Hz, and the maximum amplitude of the displacement response was measured as 75 μm. A dashed curve in Fig. 12 depicts the dynamical compliance of the beam obtained at 20 cm from the left end of the beam as will be discussed shortly. As seen from the figure, six structural modes appear in the frequency range up to 100 Hz.

Depicted in Fig. 11(b) is the displacement response of the beam at 35 Hz after ABC conducted in an effort to generate a clamped support at $x = 0.42$ m. A pair of gap sensors with the resolution of 0.1 μm were respectively implemented at $x_{s1} = 0.4$ m and $x_{s2} = 0.44$ m, while a pair of piezo ceramic actuators (Type 1 in Fig. 2) were installed at $x_{c1} = 0.05$ m and $x_{c1} = 0.2$ m. As seen from the figure, a clamped support was generated at the designated position $x = 0.42$ m. The maximum displacement of the beam was reduced to 0.95 μm, about 12% of that before ABC. Thus the objective of producing a desired boundary condition; a clamped support in this case, was accomplished experimentally via ABC. Comparing a theoretically achievable control effect shown in Fig. 5 with the experimental result in Fig. 11(b) shows a good agreement.

Next, with a view to realizing a vibration-free state in a desired region of a beam, an experiment was conducted. Fig. 11(c) shows the experimental result of a displacement response of the beam after ABC.

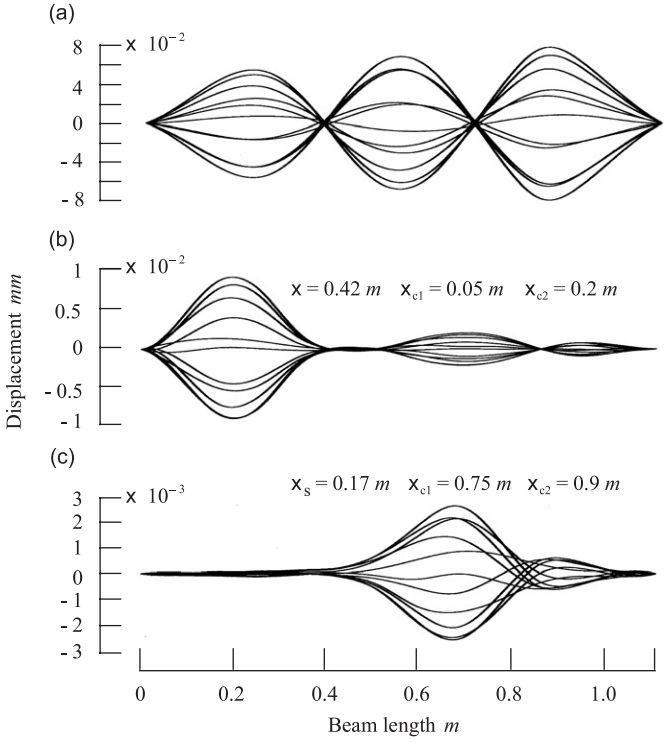

Fig. 11. Experimental results of ABC: (a) time histories of displacement response before ABC; (b) time histories of displacement response after ABC conducted to generate a clamped support at $x = 0.42$ m; and (c) time histories of displacement response after ABC for generating a completely vibration-free state.

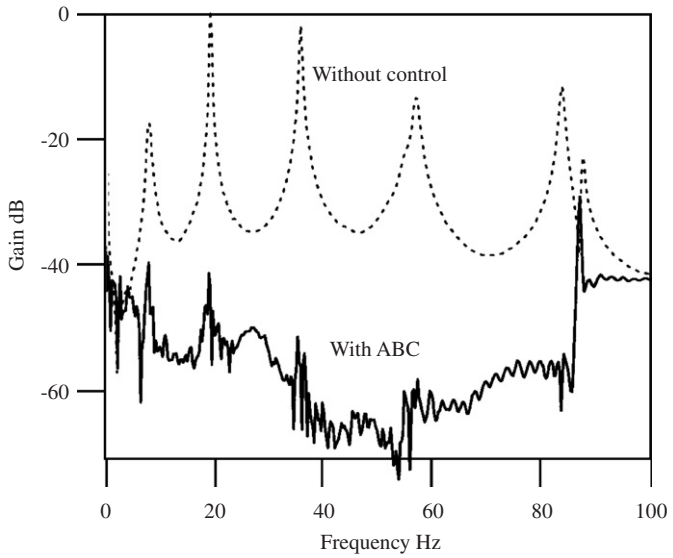

Fig. 12. Experimental results of dynamical compliances at $x = 20$ cm before and after ABC with a random excitation.

As seen from the figure, a vibration-free state in the region between the left end of the beam and the location around $x = 0.4$ m was produced. In this case, error sensors were placed at $x_{s1} = 0.17$ m and $x_{s2} = 0.21$ m, while moment actuators were moved to $x_{c1} = 0.75$ m and $x_{c2} = 0.9$ m, respectively. Unlike a simulation result, achieving a literally vibration-free state is not an easy task in practice. However, taking into account the sensor resolution (0.1 μm in this case), the power of control actuators used and the variability of a flexible beam response that is likely to be affected by environmental disturbance, the control effect shown in the figure is satisfactory. More important, the experimental results show the validity of generating a vibration-free state in a designated region of a beam via ABC.

The maximum amplitude of the beam deflection observed in the right-hand side of the controller location was reduced to 2.5 μm; only 3% of that before ABC. It should be noted that the region from the actuator location toward the right end of the beam is beyond the sphere of control as the control point is outside the area, so that when a driving frequency varies, the deflection response also changes.

Comparing the numerical simulation in Figs. 7 and 8 with the experimental result in Fig. 11(c), some discrepancies appear. In the numerical simulation, the vibration free region is generated from the left end of the beam to the actuator location at x_{c1}; in the experimental result, however, the near field effect around x_{c1} is considerably strong, with the result that the vibration free region is narrowed; from the left end of the beam to the location around $x = 0.4$ m. The reason for this is the same as stated above. In addition, the load effect due to the attachment of the piezo-ceramic actuators on the beam may be attributed to the discrepancies.

As long as active control of sinusoidal vibration as was discussed in Fig. 11 is concerned, it may be performed by a mere phase and gain adjustment of a control signal no matter what control strategy might be employed. When it comes to random vibration, it is no longer the matter of a signal manipulation but implementation of a controller dynamics in a frequency band of interest. Accordingly, difficulty as well as complexity in control immediately arises. In reality, random vibration is common so that it is worth investigating into the practicality of ABC.

Fig. 12 shows the measured dynamical compliances (acquired at 20 cm from the left end of the beam) before and after ABC obtained by exciting the beam with a random force, the driving signal of which was generated by putting a white noise signal into a low-pass filter with the cutoff frequency at 150 Hz. The experimental condition to carry out ABC was the same as was used in Fig. 11(c). As with an adaptive feedforward control set up, the specifications are as follows: digital signal processor (dSPACE 1103); 256 taps for a system identification; 128 taps for an FIR controller; sample rate is 1 kHz. Solid curve in Fig. 12 indicates the dynamical compliance after ABC. Comparing both plots in the figure, it can be seen that generation of

a perfect vibration-free state was not achieved in practice due to the same reason stated above, however even when a beam was subjected to a random force, satisfactory reduction at the control point of the beam was obtained. Thus irrespective of driving frequency varying randomly in a wide range, it is revealed that ABC enables the generation of a vibration-free state at the designated region of the beam. The maximum reduction obtained experimentally was measured as 45 dB.

6. Conclusions

In light of the fact that structural modes of a flexible beam are determined by boundary conditions, ABC (active boundary control) has been presented. ABC aims to generate a desired boundary condition at the designated location of a beam. First, the feedforward control law of the ABC system was derived using a transfer matrix method. In addition to conventional four boundary conditions, two more boundary conditions were found to be produced by ABC. Moreover, ABC enables the generation of a completely vibration-free state—neither progressive waves nor reflected waves exist—in the designated region of a beam. Finally, with a view to verifying the validity of ABC, an experiment was conducted using an adaptive feedforward control based upon a filtered-x LMS algorithm, demonstrating that ABC generates a desired boundary at a designated location of a beam, and creates a completely vibration-free state at a designated area of a beam.

References

[1] H.H. Rosenbrock, Distinctive problems of process control, *Chemical Engineering Progress* 58 (9) (1962) 43–50.
[2] L.A. Gould, M.A. Murray-Lasso, On the modal control of distributed systems with distributed feedback, *IEEE Transactions on Automatic Control* AC-11 (4) (1966) 729–737.
[3] J.D. Simon, S.K. Mitter, A theory of modal control, *Information and Control* 13 (1968) 316–353.
[4] L. Meirovitch, H. Baruh, The implementation of modal filters for control of structures, *Journal of Guidance* 8–6 (1985) 707–716.
[5] D.R. Vaughan, Application of distributed parameter concepts to dynamic analysis and control of bending vibrations, *ASME Journal of Basic Engineering* June (1968) 157–166.
[6] A.H. von Flotow, J.B. Schafer, Wave absorbing controllers for a flexible beam, *Journal of Guidance* 9–6 (1986) 673–680.
[7] G.M. Procopio, J.E. Hubbard Jr., Active damping of a Bernoulli-Euler beam via end point impedance control using distributed parameter techniques, ASME Design Technology Conference, 1987, pp. 35–46.
[8] B.R. Mace, Active control of flexural vibrations, *Journal of Sound and Vibration* 114–2 (1987) 253–270.
[9] D.W. Miller, S.R. Hall, A.H. von Flotow, Optimal control power flow at structural junctions, *Journal of Sound and Vibration* 140 (3) (1990) 475–497.
[10] D.G. MacMartin, S.R. Hall, Control of uncertain structures using an H-infinity power flow approach, *Journal of Guidance* 14 (3) (1990) 521–530.
[11] N. Tanaka, Y. Kikushima, Active wave control of a flexible beam (Proposition of the active sink method), *JSME International Journal* 34–2 (1991) 159–167.
[12] N. Tanaka, Y. Kikushima, Active wave control of a flexible beam (Fundamental characteristics of an active sink system and its verification), *JSME International Journal* 35–2 (1992) 236–244.
[13] N. Tanaka, Y. Kikushima, Optimal vibration feedback control of an Euler–Bernoulli beam: toward realization of the active sink method, *ASME,Journal of Vibration and Acoustics* 121 (1999) 174–182.
[14] R.L. Kosut, H. Salzwedel, A. Emami-Naeini, Robust control of flexible spacecraft, *Journal of Guidance* 6–2 (1983) 104–111.
[15] G. Stein, J.C. Doyle, Beyond singular values and loop shapes, *Journal of Guidance and Control* 14 (1) (1991) 5–16.
[16] S. Boyd, Linear Matrix Inequalities in System and Control Theory, SIAM Studies in Applied Mathematics, 1994.
[17] J.N. Aubrun, Theory of the control of structures by low-authority control, *Journal of Guidance and Control* 3 (1980) 444–451.
[18] M.J. Balas, Direct velocity feedback control of large space structures, *Journal of Guidance* 2–3 (1979) 252–253.
[19] M.J. Balas, Trends in large space structure control theory: fondest hopes, *Wildest Dreams, IEEE Transactions on Automatic Control* AC 27 (1982) 522–535.
[20] R.D. Joslin, R.A. Nicolaides, G. Erlebacher, M.Y. Hussaini, M.D. Gunzburger, Active control of boundary-layer instabilities: use of sensors and spectral controller, *AIAA Journal* 33 (8) (1995) 1521–1523.
[21] R.W. Metcalfe, D. Rutland, J.H. Duncan, J.J. Riley, Numerical simulations of active stabilization of laminar boundary layers, AIAA paper, 85-0567, 1985.
[22] R. Athnasingham, K. Breuer, Active control of turbulent boundary layers, *Journal of Fluid Mechanics* 495 (2003) 209–233.
[23] C.F. Baicu, C.D. Rahn, B.D. Nibali, Active boundary control of elastic cables: theory and experiment, *Journal of Sound and Vibration* 198 (1) (1996) 17–26.
[24] R. Datko, J. Lagnese, M.P. Polis, An example on the effect of time delays in boundary feedback stabilization of wave equations, *SIAM Journal of Control and Optimization* 24 (1986) 152–156.

[25] F. Contrad, O. Morgul, On the stability of a flexible beam with a tip mass, *SIAM Journal of Control and Optimization* 36 (6) (1998) 1962–1986.
[26] J. Liang, Y. Chen, B.Z. Guo, A new boundary control method for beam equation with delayed boundary measurement using modified Smith prediction, *Proceedings of the 42nd IEEE Conference on Decision and Control*, Maui, Hawaii, 2003, pp. 809–814.
[27] A. Baz, Boundary control of beams using active constrained layer damping, *Transactions of ASME, Journal of Vibration and Acoustics* 119 (April) (1997) 166–172.
[28] E.C. Pestel, F.A. Leckie, *Matrix Methods in Elastomechanics*, McGraw-Hill Book Co., New York, 1963.